

Synthesis, experimental and theoretical characterization, and field-effect transistor properties of a new class of dibenzothiophene derivatives: From linear to cyclic architectures

Yali Qiao,^a Zhongming Wei,^a Chad Risko,^b Hong Li,^b Jean-Luc Brédas,^{*bc} Wei Xu^{*a} and Daoben Zhu^{*a}

^a Beijing National Laboratory for Molecular Sciences, Key Laboratory of Organic Solids, Institute of Chemistry, Chinese Academy of Sciences, Beijing 100080, P. R. China. Fax: +86 10 62569349; Tel: +86 10 62639355; E-mail: wxu@iccas.ac.cn, zhudb@iccas.ac.cn

^b School of Chemistry and Biochemistry and Center for Organic Photonics and Electronics, Georgia Institute of Technology, Atlanta, Georgia 30332-0400, USA

^c Department of Chemistry, King Abdulaziz University, Jeddah 21589, Saudi Arabia

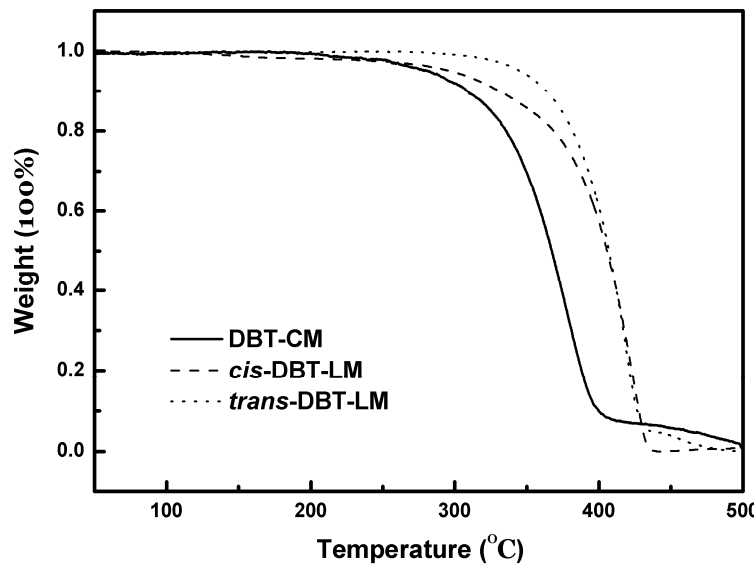


Fig. S1 Thermal gravimetric analysis (TGA) of **DBT-CM**, **cis-DBT-LM**, and **trans-DBT-LM**.

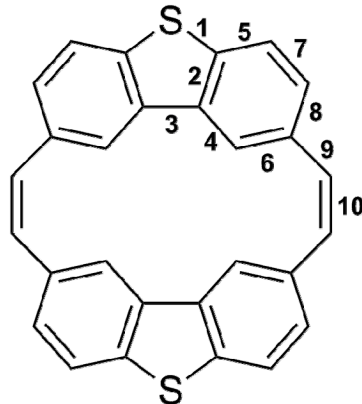


Fig. S2 The bond numbering scheme for **DBT-CM**.

Table S1 DFT (B3LYP/6-31G**) bond lengths (\AA) for the neutral (N), radical-cation (C), and radical-anion (A) states of **DBT-CM**, **cis-DBT-LM**, and **trans-DBT-LM**. The X-ray molecular bond lengths are also presented.

Bond (\AA)	expt.	B3LYP/6-31G**				
DBT-CM						
		N	C	Δ (C-N)	A	Δ (A-N)
1	1.749 (2)	1.766	1.749	-0.017	1.765	-0.001
2	1.407 (2)	1.412	1.418	0.006	1.415	0.003
3	1.456 (2)	1.459	1.463	0.004	1.465	0.006
4	1.391 (3)	1.400	1.391	-0.009	1.396	-0.004
5	1.392 (2)	1.396	1.400	0.004	1.402	0.006
6	1.394 (2)	1.403	1.414	0.011	1.416	0.013
7	1.380 (3)	1.387	1.383	-0.004	1.384	-0.003
8	1.418 (2)	1.419	1.424	0.005	1.430	0.011
9	1.470 (3)	1.471	1.453	-0.018	1.449	-0.022
10	1.352 (2)	1.358	1.373	0.015	1.383	0.025
cis-DBT-LM*						
1	1.749 (2)	1.765	1.734	-0.031	1.780	0.015
2	1.409 (4)	1.412	1.427	0.015	1.420	0.008
3	1.444(4)	1.456	1.457	0.001	1.457	0.001
4	1.397 (4)	1.400	1.386	-0.014	1.392	-0.008
5	1.393 (4)	1.397	1.408	0.011	1.399	0.002
6	1.396 (4)	1.401	1.419	0.018	1.422	0.021
7	1.380 (5)	1.388	1.378	-0.010	1.386	-0.002
8	1.408 (4)	1.415	1.429	0.014	1.441	0.026
9	1.472 (4)	1.474	1.437	-0.037	1.433	-0.041
10	1.335 (4)	1.350	1.382	0.032	1.398	0.048
trans-DBT-LM*						
1	1.749 (2)	1.764	1.734	-0.030	1.779	0.015
2	1.403 (3)	1.412	1.426	0.014	1.421	0.009

3	1.445 (3)	1.456	1.457	0.001	1.457	0.001
4	1.398 (3)	1.400	1.386	-0.014	1.392	-0.008
5	1.390 (4)	1.398	1.409	0.011	1.400	0.002
6	1.390 (3)	1.402	1.419	0.017	1.422	0.020
7	1.380 (3)	1.387	1.376	-0.011	1.385	-0.002
8	1.414 (3)	1.417	1.429	0.012	1.441	0.024
9	1.462 (3)	1.465	1.432	-0.033	1.428	-0.037
10	1.334 (3)	1.349	1.378	0.029	1.392	0.043

*Due to the asymmetric substitution of the **DBT** units in **cis-DBT-LM** and **trans-DBT-LM**, the bond lengths within each **DBT** unit are slightly asymmetric; for instance, the other sulfur-carbon bond is 1.753 (3) in **cis-DBT-LM** and 1.753 (2) in **trans-DBT-LM**.

Table S2 Vertical and adiabatic ionization potential (VIP and AIP, respectively) and electron affinity (VEA and AEA, respectively) energies, and HOMO and LUMO energies as determined at the B3LYP/6-31G(d,p) level of theory. All energies in eV. The dibenzothiophene (**DBT**) monomer is included for comparison.

	AIP	VIP	AEA	VEA	HOMO	LUMO
DBT	7.50	7.57	0.54	0.70	-5.83	-0.96
DBT-CM	6.43	6.50	-0.47	-0.37	-5.27	-1.59
cis- DBT-LM	6.50	6.65	-0.25	-0.03	-5.43	-1.27
trans- DBT-LM	6.39	6.50	-0.32	-0.20	-5.29	-1.44

Table S3 Relaxation energy for the ground (λ_1) and radical-ion (λ_2) states, and total intramolecular reorganization energies for oxidation and reduction ($\lambda_{\text{r}}(\text{ox})$ and $\lambda_{\text{r}}(\text{red})$, respectively) determined via the adiabatic potential energy surface and normal mode approach (in parentheses) at the B3LYP/6-31G(d,p) level of theory. All energies in eV. The dibenzothiophene (**DBT**) monomer is included for comparison.

	holes			electrons		
	λ_1	λ_2	$\lambda_{\text{r}}(\text{h})$	λ_1	λ_2	$\lambda_{\text{r}}(\text{e})$
DBT	0.066 (0.065)	0.064 (0.067)	0.130 (0.132)	0.154 (0.158)	0.153 (0.148)	0.307 (0.306)
DBT-CM	0.077 (0.077)	0.074 (0.074)	0.151 (0.151)	0.099 (0.097)	0.101 (0.102)	0.200 (0.199)
cis- DBT-LM	0.168 (0.158)	0.152 (0.201)	0.320 (0.359)	0.219 (0.208)	0.216 (0.388)	0.435 (0.596)
trans- DBT-LM	0.118 (0.117)	0.110 (0.112)	0.228 (0.229)	0.141 (0.144)	0.124 (0.130)	0.265 (0.274)

Table S4. Excited-state vertical transition energies (E , eV) and wavelengths (λ , nm), oscillator strengths (arbitrary units), and excited-state electronic configurations as determined with TDDFT at the B3LYP/6-31G(d,p) level of theory.

	E_{opt} (eV)	λ_{opt} (nm)	f	Configuration
DBT-CM	4.01	310	1.02	HOMO-1→LUMO (50%); HOMO→LUMO+3 (24%); HOMO→LUMO+1 (6%); HOMO-2→LUMO+2 (3%)
cis- DBT-LM	3.71	335	0.32	HOMO→LUMO (73%); HOMO→LUMO+1 (15%); HOMO-2→LUMO (2%)
	3.81	325	0.47	HOMO→LUMO+1 (65%); HOMO→LUMO (15%); HOMO-2→LUMO (10%)
trans- DBT-LM	3.56	348	1.14	HOMO→LUMO (78%); HOMO→LUMO+2 (6%); HOMO-2→LUMO (2%)
	3.78	328	0.38	HOMO→LUMO+2 (73%); HOMO-2→LUMO (12%); HOMO→LUMO (6%); HOMO-4→LUMO (2%)

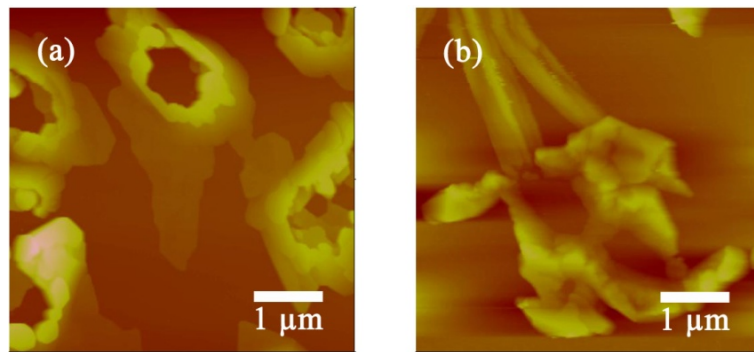


Fig. S3 AFM images of 50-nm-thick thin films of the two linear isomers vacuum deposited on OTS treated SiO₂/Si substrates at 60 °C: (a) for compound *cis*-DBT-LM and (b) for compound *trans*-DBT-LM. The scale of each AFM image is 5 μm × 5 μm.

Copies of ^1H NMR and ^{13}C NMR spectra

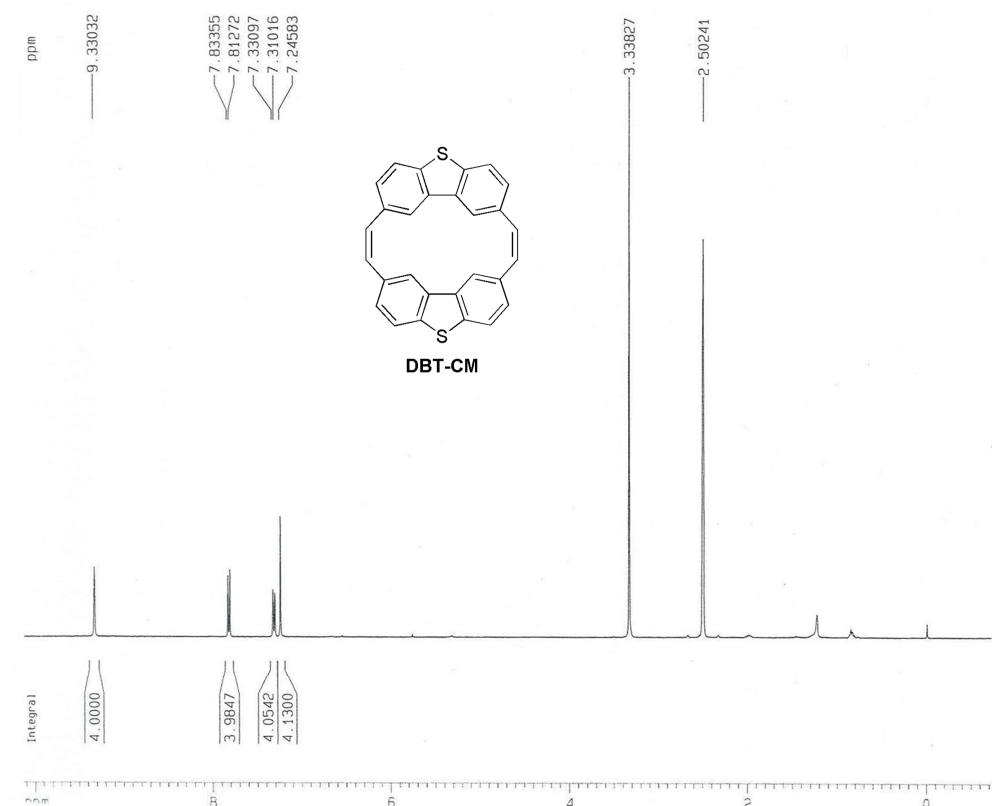


Fig. S4 ^1H NMR spectrum of DBT-CM.

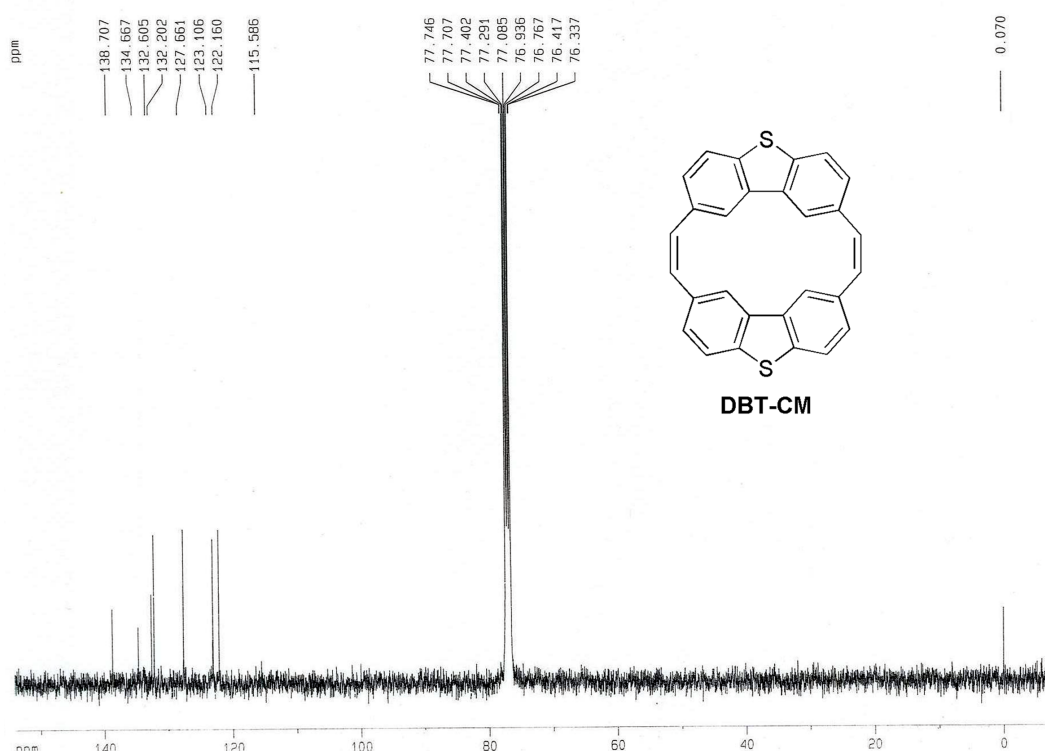


Fig. S5 ^{13}C NMR spectrum of DBT-CM.

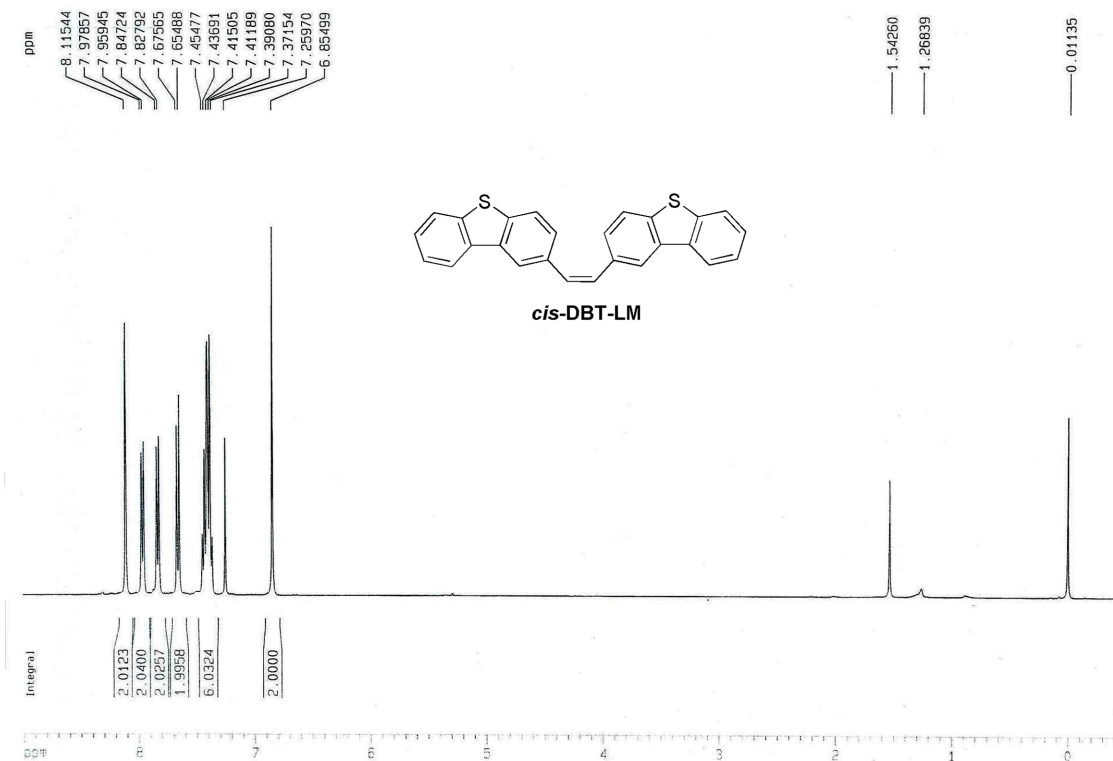


Fig. S6 ¹H NMR spectrum of *cis*-DBT-LM.

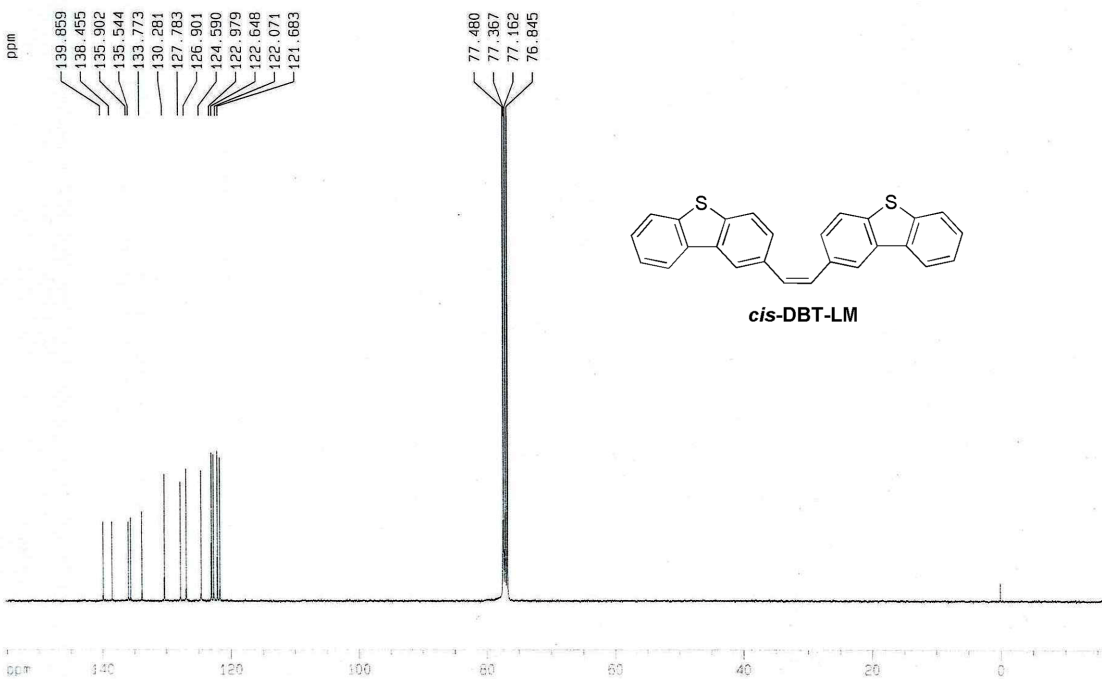


Fig. S7 ¹³C NMR spectrum of *cis*-DBT-LM.

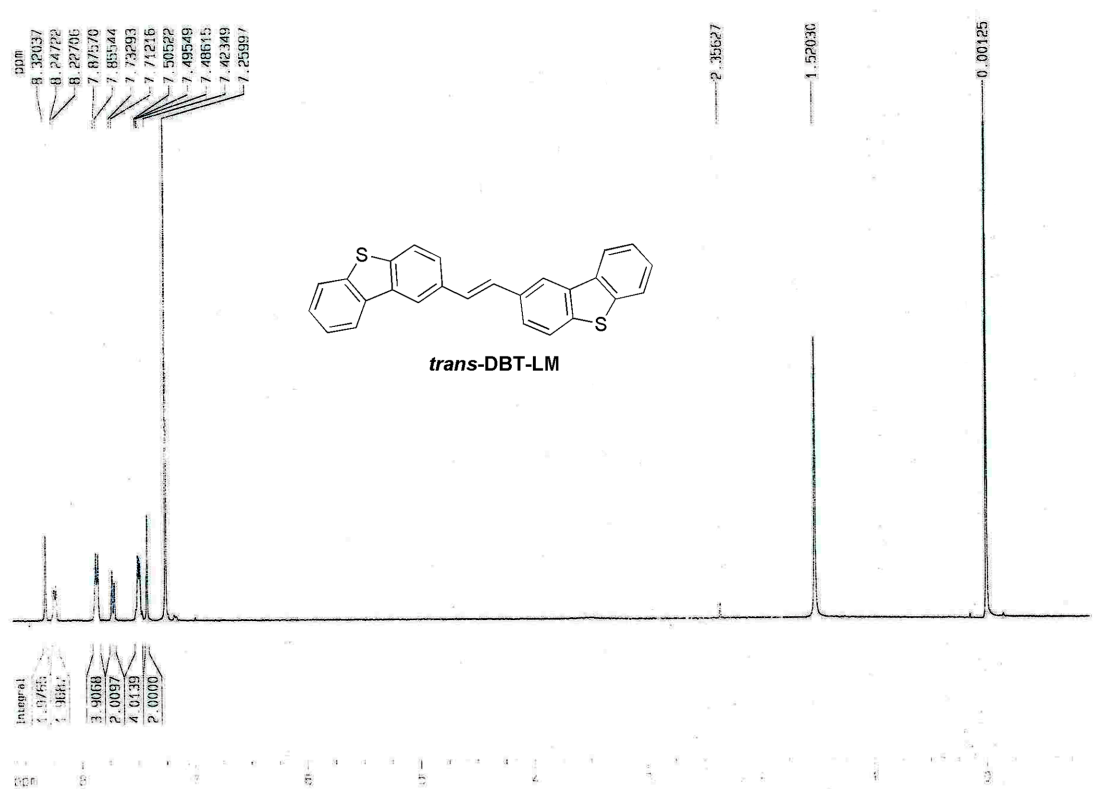


Fig. S8 ^1H NMR spectrum of *trans*-DBT-LM.